

**9th International Symposium on New Materials and Nano-Materials for  
Electrochemical Systems  
XII International Congress of the Mexican Hydrogen Society  
Merida, Mexico, 2012**

**Theoretic-Experimental Study of Pd-based Electrocatalysts for Fuel Cells**

G. Ramos-Sánchez ‡, R. Grande-Atzatzi, O. Solorza-Feria\*, A. Vela

<sup>1</sup>Depto. Química, Centro de Investigación y de Estudios Avanzados del IPN,  
Av. Instituto politécnico nacional No. 2506. Col. San Pedro Zacatenco 07360 México D.F.

\*Tel: (+52) 55 57473715, ‡ mail: [gramos@cinvestav.mx](mailto:gramos@cinvestav.mx)

**ABSTRACT**

The electrochemical oxygen reduction reaction (ORR) was analyzed by both theoretic and experimental methods, the objective of this project is to elucidate the factors controlling the observed activity and be able to design electrocatalysts ad hoc with high activity and stability. Three electrocatalysts were studied: Pd, PdNi and PdSe. For the theoretical study was used DFT as implemented in the deMon 2K software, oxygen adsorption was calculated in a four atoms cluster and then reduction steps were calculated. In this study we found that there are remarkable differences in the adsorption process for example: The oxygen adsorption energy is higher in PdNi followed by Pd and very low in PdSe, the preferred type of oxygen adsorption is bridge on Pd and PdNi however in PdSe the preferred adsorption is 1-hapticity on a single Pd atom. The experimental study demonstrate high activity towards the ORR when PdNi is used as catalyst, lesser for Pd and very low activity for PdSe, it was also demonstrated high hydrogen peroxide production on PdSe and low production on Pd and PdNi.

The theoretical and experimental results match very well correlating the Oxygen adsorption with the electrochemical activity and the species formed during the simulation with the ORR mechanism.



## **1. Introduction**

As electrochemical devices that directly convert fuels into electricity, fuel cells have some intrinsic properties that made them very attractive. Some of them are high energetic efficiency, no pollutants emission, noiselessly operation and modular capacity [1]. However, intensive research is needed to find better catalyst able to drive the normally slow Oxygen Reduction Reaction (ORR) kinetics [2].

Many approaches have been proposed in order to eliminate or decrease the use of platinum in fuel cells, platinum alloys or core shell compounds [3-4], palladium alloys or Pd/Pt core shell [5,6], Ru chalcogenides [7] and non-noble compounds [8,9]. The challenge of produce new catalyst is difficult, it isn't easy to find a new material with high catalytic activity, high selectivity, high stability and durability and for sure lower price [10].

It is undoubtedly that theoretic studies have helped to deeper understanding of the process occurring in fuel cells and also have served as start point for electrocatalyst synthesis [11-12]. Beyond the theoretical approach have been reported other studies in which the theoretical approach is carried out together with experimental studies [13-14].

In this work extensive electrochemical and first studies on theoretic Oxygen reduction in Pd, PdNi and PdSe, materials that has been proposed as catalyst for use in the cathode of low temperature fuel cells.

## **2. Experimental**

### **2.1 Synthesis and physicochemical characterization**

Pd and PdNi were synthesized by a widely reported reduction process [15]. Briefly 0.11 mmol PdCl<sub>2</sub> were dissolved in 100 ml THF and flurried during 24 h, after that 0.22 mmol NaBH<sub>4</sub> were quickly added and flurried during 0.5 h. The obtained powder was decanted washed with water and dried in N<sub>2</sub> atmosphere at 70 °C during 6 h. The same procedure was used for the PdNi synthesis, except with the addition of 0.11 mmol NiCl<sub>2</sub> and double solvent amount. The PdSe compound was synthesized by the decomposition of a Pd<sub>x</sub>(CO)<sub>y</sub> compound in the presence of Se at 230 °C in 1,6 hexanediol. The obtained powder was decanted, washed thoroughly with ethyl-ether and dried.

The synthesized compounds were analyzed by Transmission Electron Microscopy (TEM) with a JEOLJEM 1200 EXM microscopy operated at 1200 kV and 70 µA. X-Ray diffraction (XRD) was used to analyze phases, an D8 Advance equipment from Brucker was used with CuKα (λ=0.154056 nm) from 30 to 90° in 2θ, the composition was analyzed with an Energy dispersive X-ray (EDX) Genesis 4000 equipment.

For the electrochemical experiments an ink with the catalytic material was prepared and deposited onto a 3mm diameter glassy carbon with Teflon® holder electrode. The ink was prepared by mixing 1 mg of the synthesized material and 1 mg of carbon Vulcan® then was added 6 µl of Nafion® at 5% (Aldrich) and 50 µl of isopropyl alcohol. The mixture was sonicated during 15 min, 2 µl of the resulted suspension was collocated on the exposed carbon surface of the electrode. For the experiments a classic three electrode array was used, the work electrode prepared as previously stated, a Pt mesh as counter-electrode, and a Hg/Hg<sub>2</sub>SO<sub>4</sub>/0.5 M H<sub>2</sub>SO<sub>4</sub> reference electrode

**9th International Symposium on New Materials and Nano-Materials for  
Electrochemical Systems  
XII International Congress of the Mexican Hydrogen Society  
Merida, Mexico, 2012**

(0.68 V vs NHE).  $\text{H}_2\text{SO}_4$  0.5 M was used as electrolyte and during the experiments  $\text{N}_2$ ,  $\text{O}_2$  or CO was bubbled in the electrolyte.

## 2.2 Theoretic study

All the calculations were made with the functional density theory (DFT) and the lineal combination of Gaussian type orbitals to solve the Khon-Sham Equations as implemented in the demon 2k software version 2.4.4 [16]. The geometry optimization was done within the approximation of generalized gradient approximation (GGA) with the exchange-correlation functional of Perdew-Becke-Ernzerhoff (PBE) [17].

For the ORR simulation a metallic cluster was used as the catalyst and different intermediates of the ORR were induced to interact with the cluster ( $\text{O}_2$ , OH, OOH,  $\text{H}_2\text{O}_2$  and  $\text{H}_2\text{O}$ ). The analyzed clusters were  $\text{Pd}_4$ ,  $\text{Pd}_2\text{Ni}_2$ , and  $\text{Pd}_2\text{Se}_2$  in different electronic states. For H<sub>2</sub>O and Se the double  $\xi$  orbital with polarization functions base was used, for Pd the 18 electrons pseudopotential and quasirelativistic ECP|SD base from Stuttgart-Dresden was used, and for Ni the pseudopotential and non-relativistic base ECP|SD base was used. All optimizations were done without symmetry constrains unless otherwise stated.

## 3. Results and discussion

The structural parameters of the three compounds are resumed in Table 1. Images and spectra are available in the supplementary information.

Table 1. Structural parameters of Pd, PdSe and PdNi compounds.

Electrocatalyst	Particle size (TEM) / nm	Crystallite size / nm	Composition (EDX)
Pd	4	7	100
PdNi	4-10	9	37:62
PdSe	20	10	51:49

The obtained electrocatalyst powder show agglomeration because of the lack of support, however the formation of nanometric particles is evident by booth microscopic and diffraction experiments. The XRD diffractogram corresponds in the case of Pd and PdNi to the diffraction peaks of Pd fcc, in the case of PdNi those peaks are shifted towards more positive values in  $2\theta$ , indicating the formation of the PdNi alloy. For PdSe the XRD experiment revealed many intermetallic compounds with different stocquiometry that has been up to now impossible to identify or isolate. The calculated composition is very close to that expected for PdSe but very different in PdNi in which there is a high quantity of Ni in the alloy.

The electrochemical characterization showed specific current-potential behavior for every electrocatalyst. Cyclic voltammetry was performed in nitrogen saturated electrolyte (Fig 1), the voltage scan start in the open circuit

potential ( $\sim 0.8$  V) in anodic direction to 0V, followed by the cathodic scan up to 1.4 V. The voltammogram for Pd has been widely reported [18] in the figure 1 this behavior is observed, the hydrogen adsorption-desorption process (0-0.3V), the process of formation of oxides and de subsequent reduction in a peak at 0.6 V. The voltammogram of PdNi is very similar to that of Pd, however is remarkable that the peak reduction is shifted towards more positive potentials 0.7 V indicating an easier reduction process. For the PdSe electrocatalyst the voltammogram is very different, the hydrogen adsorption-desorption process is completely absent, the reduction of oxides is now shifted but to more negative potentials (0.52 V) indicating a more difficult reduction process.

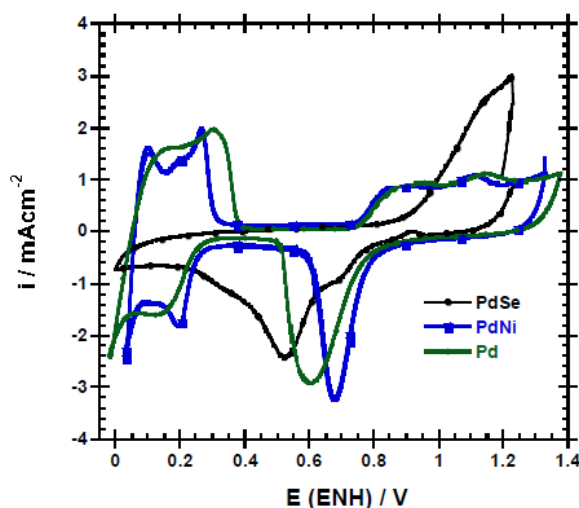


Figure 1. Cyclic voltammogram of Pd, PdNi and PdSe.  $v=50 \text{ mVs}^{-1}$  in  $\text{H}_2\text{SO}_4$  0.5 M saturated with Nitrogen.

The kinetic of the ORR was studied by RDE experiments, this experiment was done in oxygen saturated electrolyte with electrode rotating from 100 to 2500 rpm and very slow voltage scan ( $v=5 \text{ mVs}^{-1}$ ). The resulted data were corrected to eliminate the mass transfer process following the procedure described by Levich [19], in order to construct the Tafel plots for the electrocatalyst PdNi (Fig. 2a) and PdSe (Fig. 2b), booth figures compare the electrocatalyst with Pd in order to observe the differences.

The Tafel plots of PdNi indicate a more positive open circuit potential as well as higher current at the same potential on the other hand, for PdSe the open circuit potential is lesser positive and is needed a high overpotential to reach the same current density. In other words the catalytic activity is higher for PdNi and lower for PdSe in comparison with that presented by Pd. This result could be related also with position of the reduction of oxides in the cyclic voltammetry.

Rotating Ring disk electrode experiments showed a high hydrogen peroxide production on the PdSe electrocatalyst. In Pt and Pt-based electrocatalyst the peroxide production is very low  $<2\%$ , which indicates that because of the

presence of Se, probably the oxygen adsorption is very weak, leading a very O-O bond which originates a high peroxide production as it has been probed in the oxygen reduction with gold electrodes [20].

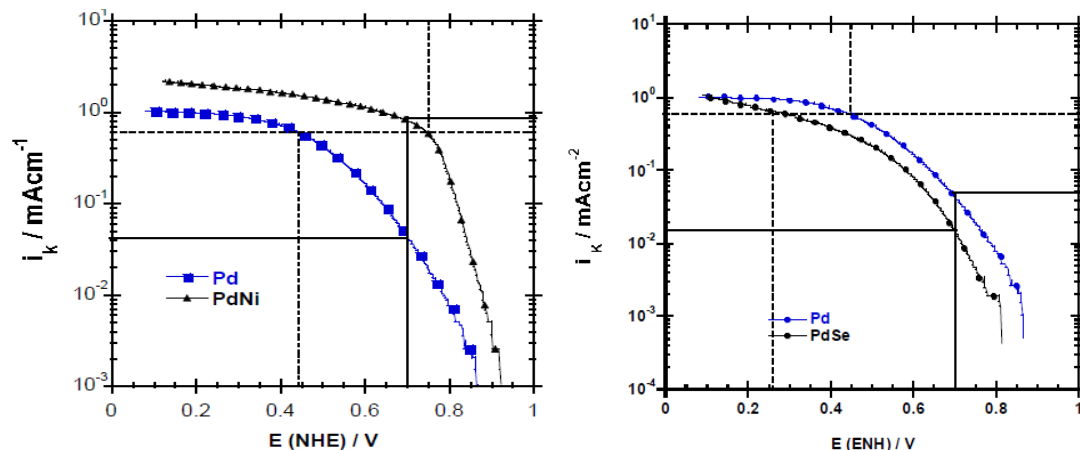


Figure 2. Mass transfer corrected Tafel plots for a) PdNi and b) PdSe. Plots made from de RDE experiments.

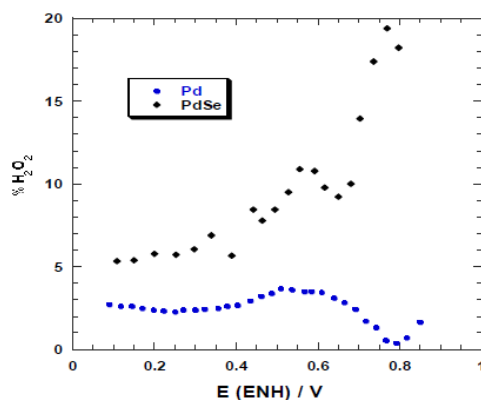


Figure 3. Hydrogen peroxide production versus potential, from RRDE experiments. Catalytic ink in the disc with voltage scan from ocp to 0V,  $v=10 \text{ mVs}^{-1}$ . Gold ring at 1.4 V, in  $\text{H}_2\text{SO}_4$  0.5 M.


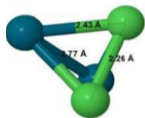
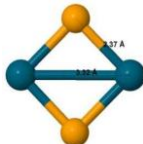
The electrochemical experiments have helped to the characterization and deeper understanding of the processes happening in the different electrocatalyst; however up to now it doesn't give any clue about the way to synthesis a better catalyst. This study up to now just give us the intrinsic properties of the catalysts, to give the next step we decided to study the ORR by theoretical methods.

The approach for the simulation of the solid is the cluster one. In table 2 we report the optimized clusters used for the simulation as well as some energetic and structural data. The optimization procedure consisted in find the lower energy structure for different conformations and multiplicities. It is easily observed that the PdNi cluster retains the

**9th International Symposium on New Materials and Nano-Materials for  
Electrochemical Systems  
XII International Congress of the Mexican Hydrogen Society  
Merida, Mexico, 2012**

connectivity of the Pd cluster but enlarging the Pd-Pd bond length and shorting the PdNi bond length. The lowest energy structure corresponded to a multiplicity of 3 in the three cases.

Table 2. Clusters used for the ORR simulation. Blue balls Pd, green Ni and Se in yellow.

Electrocatalyst	$\Delta\text{Dis} /$ $\text{kcal mol}^{-1}$	$\epsilon_{\text{coh}} /$ $\text{kcal mol}^{-1}$	HOMO-LUMO / $\text{kcal mol}^{-1}$	Bond length/ Å
	155.7	39.4	35	PdPd: 2.57 PdPd: 2.63
	191.2	47.8	27.5	PdPd: 2.77 NiNi: 2.26 PdNi: 2.43
	216.2	54.1	24.49	PdPd: 3.32 SeSe: 3.39 PdSe: 2.37

Energetic data as dissociation energy ( $\Delta\text{Dis}$ ) and cohesive energy ( $\epsilon_{\text{coh}}$ ) are calculated according to the procedure reported by Ahlrichs [21], those values the stability of the cluster, as the dissociation energy rises is more difficult to break the cluster away, the same applies for the cohesive energy. In this sense the new bimetallic clusters have higher stability which represents advantages for its use in the very reactive environment present in fuel cells. The HOMO-LUMO is reported because some authors [22] have speculated that this parameter is linearly related to the catalytic activity, speculation that is not observed in this study.

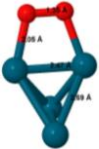
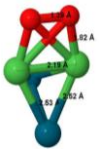
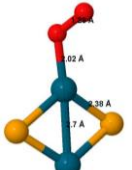
Once the lower energy clusters are obtained they are used for the adsorption of oxygen. Many structures are possible owed to the different adsorption sites, geometries and multiplicities, however the lower energy structure is searched and reported in table 3. The lowest energy structure suggests that that is the specie that is likely to exist, however other species could also be formed because they are minima in the process. A molecular dynamic study is needed and would complete the methodology proposed in this work.

For the oxygen adsorption the lowest structure corresponds to a bridge adsorption, the same is observed for the PdNi cluster; however, the oxygen is preferred bonded to the Ni atoms. In the PdSe cluster, in the other hand, the most stable adsorption site a single Pd atom single-coordinated to an oxygen atom. All structures correspond to a triplet, however the energetic differences are remarkable: a very low adsorption energy for oxygen on PdSe and high adsorption energy on the PdNi cluster. This trend was observed in the experimental studies which indicate that this parameter is related to the catalytic activity as it's been proposed by many authors [13, 23-24].



**9th International Symposium on New Materials and Nano-Materials for  
Electrochemical Systems  
XII International Congress of the Mexican Hydrogen Society  
Merida, Mexico, 2012**

Table 3. Oxygen adsorption properties on Pd clusters. Pd in blue, Ni in green, Se in yellow and oxygen in red..

Adsorption geometry	Adsorption energy / kcal mol <sup>-1</sup>	Bonde lenght / Å
	-31.04	PdPd: 2.47 OO: 1.35 PdO: 2.05
	-48.7	NiNi: 2.19 OO: 1.39 ONi: 1.82 PdPd: 2.53
	-22.6	PdPd: 2.7 OO: 1.28 PdO: 2.02

The full optimization from oxygen to water or hydrogen peroxide was accomplished for every multiplicity and cluster; however of interest fundamental is the ORR mechanism. It was found that is possible to elucidate the preferred mechanism with the calculation of the stability of the specie (OOH) related to that of the (O)(OH) species. If the direct mechanism toward the formation of water is the main mechanism then the (O)(OH) species will be formed and will be more stable than (OOH); however if the peroxide production is the preferred mechanism, then the (OOH) will be preferentially formed. The electronic energy difference for those process in Pd is 12.43 kcalmol<sup>-1</sup>, for PdNi this difference is 34.5 kcalmol<sup>-1</sup>, which indicates that there is a lesser probability for the formation of peroxide. On the other hand for PdSe, the only stable specie is (OOH) which indicates that the preferred mechanism is the formation of hydrogen peroxide which agrees well with the electrochemical characterization.

#### 4. Conclusions.

In this work theoretical and experimental methods were utilized to study the Oxygen reduction reaction on different Pd-based compounds. The PdNi catalytic activity is higher than that of Pd, the measured kinetic current is an order of magnitude greater than that of Pd at 0.7V, and is related to the easiest oxide reduction observed by cyclic voltammetry, the molecular simulation reflects that the oxygen adsorption energy is greater and is responsible of the

**9th International Symposium on New Materials and Nano-Materials for  
Electrochemical Systems  
XII International Congress of the Mexican Hydrogen Society  
Merida, Mexico, 2012**

measured kinetic. For PdSe in the opposite a lower catalytic activity is measured, this is attributed to the very weak oxygen adsorption energy, this weak adsorption process is also responsible for the formation of a high quantity of hydrogen peroxide.

More than the evident congruence between the theory and experiments, this work serves as start point for future studies. The theoretic methods now could be made previously to the synthesis and electrochemical characterization and then previously know the kinetic and mechanism by comparing the values of oxygen adsorption and (OOH) stability with other catalyst like Pd or Pt.

The theoretic model is simple, but correlate well with the experimental. However increasing the theory level and including factors like solvent interaction, cluster size and electrochemical potential will permit better and more quantitative comparison.

## **5. Acknowledgements**

The support of CONACYT by means of doctoral fellowship to GRS is gratefully acknowledged. The financial support for this work was provided by CONACYT and ICyTDF.

## **6. References**

- [1] W. Vielstich. Handbook of Fuel Cells Fundamentals Technology and Applications V.2., Jhon Wiley & Sons, West Sussex (2003).
- [2] S.M. Duron Torres Pilas de Combustible: principios y perspectivas. In: Gonzalez-Huerta RG, Lopez Chavez E, Velazquez Morales B, editores. Hidrogeno, Introduccion a la energia Limpia, Mexico: Universidad Autonoma de La Ciudad de Mexico; (2009)
- [3] H. Zhu, X. Li, F. Wang. Int J Hydrogen Energy, 36, 9151 (2011).
- [4] V.R. Stamenkovic, B.S. Mun, M. Arenz, K.J.J. Maryhoffer, C.A. Lucas, G. Wang, P.N. Ross, N.M. Markovic. Nature, 6, 241 (2010):
- [5] P. Mani, R. Srivastava, P. Strasser. J Power Sources, 196, 666 (2011).
- [6] V.L. Nguyen, M. Ohtaki, T.D. Hien, J. Randy, M. Nogami. Electrocchim Acta, 56, 9133 (2011).
- [7] K. Suarez-Alcantara, O. Solorza-Feria O. J Power Source2, 192, 165 (2009).
- [8] L. Wang, L. Zhang, J. Zhang. Electrochem Acta 56, 5488 (2011).
- [9] X. Li, G. Liu, B.N. Popov. J Power Sources 195, 6373 (2010)
- [10] H.A. Gasteiger, S.S. Kocha, B. Sompalli, F.T. Wagner. Appl Catal B Environment 6, 9 (2005)
- [11] Y. Suga. Chem Lett., 35, 1406 (2006)
- [12] A.B. Anderson, T.V. Albu. J Electrochem Soc., 147, 4229 (2000)
- [13] V. Stamenkovic V, B.S. Mun, K.J.J. Maryhofer, P.N. Ross, N.M. Markovic, J. Rossmeisl, J. Greeley, J.K. Nørskov. Angewandte Chem., 45, 2897 (2006).





**9th International Symposium on New Materials and Nano-Materials for  
Electrochemical Systems  
XII International Congress of the Mexican Hydrogen Society  
Merida, Mexico, 2012**

- [14] P. Rodriguez, N. Garcia-Araez, A. Koverga, S. Frank, M.T.M. Koper. *Langmuir* 26, 12425 (2010)
- [15] G. Ramos-Sanchez, O. Solorza-Feria O. *Int J Hydrogen Energy* 35,12105 (2010)
- [16] Koster AM, Calaminici P, Casida ME, Flores-Moreno R, Geudtner G, Goursot A, Heine T, Ipatov A, Janetzko F, Campo JMD, Patchkovskii S, Reveles JU, Salahub DR, Vela A, 2.3.1 ed. deMon developers: 2006.
- [17] J. P. Perdew, K. Berke, M. Ernzerhof. *Phys Rev Lett.*, 77,3865 (1996).
- [18] J.J. Salvador-Pascual, S. Citalan-Cigarroa, O. Solorza-Feria. *J Power Sources* 172,229 (2007).
- [19] L. Sung-Jai, P. Su-II, L. Sang-Kwon , K. Suk-Joong. *Isr J Chem.*, 48,215 (2008)
- [20] G. Vazquez-Huerta, G. Ramos-Sanchez, A. Rodriguez-Castellanos, D. Meza-Calderon, R. Antano-Lopez, O. Solorza-Feria. *J Electroanal Chem.*, 645, 35 (2010).
- [21] P. Nava, M. Sierka, R. Ahlrichs, *Physical Chemistry Chemical Physics* 5,3372 (2003).
- [22] T.J. Dhillip Kumar, C. Zhou, H. Cheng, R.C. Forrey, N. Balakrishnan. *J chem. Phys.*, 128, 124704 (2008).
- [23] Y. Wang, P. Balbuena. *J Chem Theory Comput.*, 1,935 (2005).
- [24] P.B. Balbuena, D. Altomare, N. Vadlamani, S. Bingi, L.A. Agapito. *J Phys Chem A*, 108,6378 (2004)